Published in final edited form as:
Angiogenesis. 2013 April ; 16(2): 279–287. doi:10.1007/s10456-012-9319-4.

PET/SPECT Imaging of Hindlimb Ischemia: Focusing on Angiogenesis and Blood Flow

Hakan Orbay[1], **Hao Hong**[1], **Yin Zhang**[2], and **Weibo Cai**[1,2,3,*]

[1]Department of Radiology, University of Wisconsin - Madison, WI, USA

[2]Department of Medical Physics, University of Wisconsin - Madison, WI, USA

[3]University of Wisconsin Carbone Cancer Center, Madison, WI, USA

Abstract

Peripheral artery disease (PAD) is a result of the atherosclerotic narrowing of blood vessels to the extremities, and the subsequent tissue ischemia can lead to the up-regulation of angiogenic growth factors and formation of new vessels as a recovery mechanism. Such formation of new vessels can be evaluated with various non-invasive molecular imaging techniques, where serial images from the same subjects can be obtained to allow the documentation of disease progression and therapeutic response. The most commonly used animal model for preclinical studies of PAD is the murine hindlimb ischemia model, and a number of radiotracers have been investigated for positron emission tomography (PET) and single photon emission computed tomography (SPECT) imaging of PAD. In this review article, we summarize the PET/SPECT tracers that have been tested in the murine hindlimb ischemia model as well as those used clinically to assess the extremity blood flow.

Keywords

hindlimb ischemia; peripheral artery disease (PAD); angiogenesis; positron emission tomography (PET); single photon emission computed tomography (SPECT); molecular imaging

Introduction

Peripheral arterial disease (PAD) is predominantly a disease of the elderly population and the incidence rate is increasing as the western world population continues to age. Prevalence of PAD in asymptomatic adults over 40 years old is 4.2% in the United States, which can be as high as 7.0% in those with metabolic syndrome [1]. PAD is a consequence of systemic atherosclerosis that leads to progressive narrowing of the arteries to many different organs, and the circulation of the lower extremities is the most frequently involved [1]. As a compensatory response to ischemia, the human body upregulates the expression of angiogenic growth factors, such as vascular endothelial growth factor (VEGF), fibroblast growth factor (FGF), hepatocyte growth factor (HGF), and the corresponding receptors that collectively can stimulate the development of collateral vessels [2]. In cases that these biological compensatory mechanisms fail (which usually do), therapeutic interventions such as exercise training, surgical bypass grafting, exogenous growth factors, gene/stem cell

Requests for reprints: Weibo Cai, PhD, Departments of Radiology and Medical Physics, School of Medicine and Public Health, University of Wisconsin - Madison, 1111 Highland Ave, Room 7137, Madison, WI 53705-2275, USA. Fax: 1-608-265-0614; Tel: 1-608-262-1749; wcai@uwhealth.org.

Competing Interests
The authors have declared that no competing interest exists.

therapies, and drug delivery systems can be used to help the reconstitution of extremity blood circulation [3, 4]. Surgical revascularization is still the best treatment for PAD, however other strategies can be considered when, for whatever reason, a surgical procedure is not possible [5].

The biological responses to therapeutic intervention should be evaluated with objective and quantitative measures in order to accurately evaluate the efficacy of the procedure. Traditional imaging techniques such as Doppler ultrasonography, magnetic resonance imaging (MRI), and contrast angiography are commonly used to assess extremity ischemia in human subjects [3, 6, 7]. Laser Doppler perfusion imaging is an efficient and inexpensive technique to document extremity ischemia without exposure to radiation (Fig. 1) [7]. However, although this technique can be useful for detecting superficial flow deficits, it is incapable of providing reliable information on subtle changes in blood flow which makes it inadequate to visualize, quantify, and characterize angiogenesis in response to ischemia [7]. MRI has good spatial resolution and tissue penetration of signal without the use of ionizing radiation, yet it is quite expensive and has much lower sensitivity for molecularly targeted imaging than nuclear medicine techniques such as positron emission tomography (PET) and single photon emission computed tomography (SPECT) [8]. Angiography can give excellent resolution, but it is highly observer dependent and not very reproducible [9, 10]. Furthermore, invasiveness and requirement for high technical expertise make this technique impractical for serial imaging.

PET and SPECT are noninvasive, radioisotope-based techniques that can be used to image changes in extremity blood circulation, which can provide early, sensitive, and specific detection of ischemic diseases at the molecular level [11, 12]. Traditionally, extremity ischemia and subsequent angiogenesis in animal models have been evaluated by highly invasive techniques that require the collection, and often the destruction, of tissue samples, which has limited clinical relevance and prohibits serial monitoring of the biologic processes in living animals. The recent development of dedicated small animal PET and SPECT imaging systems enabled the noninvasive visualization of angiogenesis via various molecularly targeted radiotracers [13–15]. Over the last decade, high resolution PET/SPECT scanners continued to be developed and made available for imaging small animals, improving the capacity for in vivo studies in mice, primates, and humans. This will facilitate cross-species comparisons, critical for successful translational research studies and optimal benefit from research using experimental model systems.

Continuous search has led to the development of several animal models of PAD [16]. Among them, the murine hindlimb ischemia model is a well-established and commonly used preclinical model for PAD [17]. When compared to other models of tissue ischemia, the murine hindlimb ischemia model offers simple surgical procedure, ease of access to the femoral artery, low mortality rate, among others [18]. In this review article, we summarize the PET/SPECT tracers that have been tested in the murine hindlimb ischemia model as well as those used clinically to assess the extremity blood flow.

Clinical Perspective

Molecular imaging can noninvasively visualize, characterize, and quantify the cellular and subcellular biological changes that occur during the development processes of various diseases [19, 20]. Among all the molecular imaging modalities, PET and SPECT are of the greatest clinical relevance because these techniques can monitor the delicate alterations during pathological processes with high sensitivity and good tissue penetration of the signal [19, 21–25]. Furthermore, combining anatomic (e.g., CT or MRI) with functional (e.g., PET and SPECT) imaging can be synergistic and yield more accurate results. When compared to

the traditional imaging methods for PAD, molecular imaging methods come into prominence because of noninvasiveness and easy applicability, which enables serial imaging of the same subject. Such serial molecular imaging studies can provide quantitative information about disease progression, aid in the evaluation of therapeutic interventions, and enable individualized monitoring of PAD patients in the clinic. The performance of a molecular imaging agent is dependent on many factors such as the size, composition, density of targeting ligands, hydrophilicity/hydrophobicity, circulation half-life, among many others [19]. Although exposure of patients to ionizing radiation is a concern for the clinical use of PET and SPECT [26], these techniques have been routinely used in the clinic for decades with little adverse effects [27–32].

Molecular imaging of angiogenesis can be directed against non-endothelial cell targets (e.g., monocytes, macrophages, and stem cells), endothelial cell targets (e.g., growth factor receptors, integrins, CD13, and cell adhesion molecules), extracellular matrix proteins, proteases, among others (Table 1) [12, 33–36]. Among the proteins involved in angiogenesis, VEGF is a highly potent and predominant angiogenic factor [37, 38]. Integrins have also been implicated in a number of processes related to angiogenesis, including cell adhesion, migration, proliferation, differentiation, and survival [15, 26, 33].

PET Imaging of Hindlimb Ischemia

Integrin $\alpha_v\beta_3$ is an intensively studied biological modulator of angiogenesis [39]. Almutairi et al. developed a biodegradable, ^{76}Br labeled, integrin $\alpha_v\beta_3$ targeted, dendritic nanoprobe for PET imaging of angiogenesis in the ischemic mouse limb [40]. Cyclic arginine-glycine-aspartic acid (RGD) motifs conjugated at the terminal ends of the nanoprobe enhanced the binding affinity to integrin $\alpha_v\beta_3$, which led to significantly increased uptake of the nanoprobe in the ischemic hindlimb between days 3 and 14, with a peak at day 7 after the surgical procedure (Fig. 2a). The circulation half-life of the nanoprobe (which contains many tyrosine residues for efficient labeling with ^{76}Br) could be adjusted within a wide range (1.4 ± 0.4 h to 50 ± 10 h), by selecting the appropriate level of dendritic branching and length of the polyethylene oxide chain. It was suggested that the nanoprobes used in this study isolated and protected the radiolabel from being rapidly recognized and metabolized.

In another study, a cyclic peptide containing the RGD motif was labeled with ^{68}Ga (termed ^{68}Ga-NOTA-RGD, where NOTA denotes 1,4,7-triazacyclononane-N,N′,N″-triacetic acid) for PET imaging of angiogenesis in the murine hindlimb ischemia model, which exhibited significant uptake in the operated limb on day 7 after the induction of ischemia [41]. The short decay half-life of ^{68}Ga (68.3 minutes) and its hydrophilic nature (in the form of Ga^{3+}) makes it a desirable radiolabel for small peptides which typically undergo rapid renal clearance. An additional advantage of ^{68}Ga over other radiolabels is the relatively low cost, since the parent nuclide ^{68}Ge has a long half-life (271 days) which allows continuous production of ^{68}Ga for more than 1 year with a ^{68}Ge generator. Another attractive feature of this method is the high stability of the ^{68}Ga-NOTA complex, which only required 10 minutes for radiolabeling at room temperature.

Natriuretic peptides are a family of heart- and vessel-derived hormones that play important roles in cardiovascular homeostasis by interacting with their corresponding natriuretic peptide receptors (NPRs) [42, 43]. The natriuretic peptide clearance receptor (NPR-C) is a potential target for PET imaging of angiogenesis, since it is the only NPR that recognizes all natriuretic peptides and natriuretic peptide fragments [44]. In a recent study by Liu et al. [44], a ^{64}Cu labeled C-type atrial natriuretic factor (CANF) fragment was investigated for PET applications. A multivalent DOTA-CANF-comb nanoprobe (where DOTA denotes 1,4,7,10-tetraazacyclododecane-1,4,7,10-tetraacetic acid and comb represents an

amphiphilic comb-like nanoparticle to which the CANF and DOTA were conjugated) was constructed which exhibited enhanced blood retention, specific activity, targeting efficiency, and uptake than the corresponding radiolabeled monovalent CANF peptide. Similar as other literature reports mentioned above [40, 41], this probe also showed a marked increase in uptake on day 7 in the ischemic hindlimb.

VEGF receptors (VEGFRs) are key regulators of angiogenesis, and activation of the VEGF/VEGFR pathway triggers multiple downstream signaling cascades that can lead to increased angiogenesis [14, 37, 45]. In one report, Willmann et al. used ^{64}Cu labeled $VEGF_{121}$ for noninvasive and quantitative monitoring of VEGFR-2 expression in the murine hindlimb ischemia model, with half of the mice in this study subjected to treadmill exercise training to enhance angiogenesis [46]. Tracer uptake in the ischemic hindlimb increased significantly after surgical creation of the model, peaked at around postoperative day 8, and gradually decreased over the following 3 weeks [46]. VEGFR-2 expression level was found to be significantly elevated in the ischemic skeletal muscle, as a result of arterial occlusion, making it a suitable target for PET imaging of angiogenesis. Taken together the literature reports to date, targeting both integrin $\alpha_v\beta_3$ and VEGFR-2 may enhance the efficiency of future PET imaging of angiogenesis in ischemia, in animal models as well as clinical investigation.

Small animal PET is capable of providing information not only about perfusion but also about the functionality of the ischemic muscle. In an interesting study, Penuelas et al. used ^{13}N-ammonia to assess the blood flow of the murine hindlimb by PET [47]. A correlation between ^{13}N-ammonia uptake and the amount of necrosis and fibrosis in the muscle tissue was observed, which reflected the functional capacity of the affected muscle tissue. Perfusion recovery was again the most prominent during the first week after surgery (Fig. 2b).

SPECT Imaging of Hindlimb Ischemia

In an early study, Hua et al. evaluated a ^{99m}Tc-labeled peptide that contains an RGD motif (NC100692, for targeting of integrin $\alpha_v\beta_3$) for in vivo imaging of angiogenesis in the murine hindlimb ischemia model [48]. The tracer exhibited rapid renal clearance from the blood, with significantly increased focal ^{99m}Tc-NC100692 activity distal to the occlusion at days 3 and 7 (Fig. 3). Of note, the binding of ^{99m}Tc-NC100692 to inflammatory or smooth muscle cells may also have contributed to the radioactivity signal in the ischemic hindlimb. Although the planar imaging method used in this study tended to underestimate the magnitude of the relative increase in ^{99m}Tc-NC100692 retention within the ischemic hindlimb, this could be corrected with the use of a higher resolution microSPECT/microCT system for tomographic instead of planar imaging.

In a subsequent study, the same group reported a semi-automated noninvasive approach for serial quantitative evaluation of peripheral angiogenesis with ^{99m}Tc-NC100692 microSPECT/micorCT imaging [49]. This semi-automated approach applied complex volumes-of-interest, derived from segmentation of the microCT images, onto the microSPECT images to calculate ischemic-to-nonischemic (I/NI) activity ratios for the proximal and distal hindlimb [49]. With this technique, high reproducibility (both intra-observer and inter-observer) and good accuracy for estimation of radiotracer activity relative to γ counting was demonstrated.

Clinical Imaging of Extremity Ischemia

PET

In general, PET imaging of extremity ischemia in human subjects aims to quantify the extremity blood flow and O_2 utilization using $C^{15}O_2$ or $^{15}O_2$ as the tracer [50–52]. In patients with unilateral neurogenic claudication, ^{15}O-labeled water has also been used to measure thigh and leg muscle blood flow with PET in response to exercise [52]. In another study, $H_2{}^{15}O$ PET scans were carried out in 17 patients to detect the muscle blood flow of legs with severe ischemia [53]. In addition, ^{18}F-2-fluoro-2-deoxy-D-glucose (^{18}F-FDG) PET has been used to quantitatively evaluate the extent and degree of active atherosclerosis in the popliteal and tibial arteries [54]. Although ^{18}F is one of the most commonly used isotopes for PET imaging [21, 55], ^{18}F labeling is typically time-consuming and laborious which hampers clinical translation of various promising PET tracers, exacerbated by the daunting regulatory hurdles and much smaller potential market for imaging of PAD when compared to PET imaging other diseases such as cancer. To date, little clinical investigation has been reported on imaging the biological processes (e.g., angiogenesis) during extremity ischemia using the molecular imaging agents described above.

SPECT

^{99m}Tc-sestamibi is a lipophilic cation which, when injected intravenously into a patient, distributes in the myocardium proportionally to the myocardial blood flow [56]. In addition to myocardial uptake, ^{99m}Tc-sestamibi is also considerably taken up by the striated muscle. Therefore, this tracer has been widely used for analyzing the muscular perfusion in various clinical settings. To visualize leg muscle perfusion both at rest and during standardized stress test using a bicycle ergometer, Bostrom et al. performed ^{99m}Tc-sestamibi SPECT in 16 patients with intermittent claudication [57]. The muscular uptake of ^{99m}Tc-sestamibi in the thigh increased significantly from rest to exercise, however the tracer uptake remained unchanged in the calf muscle. A linear correlation between the increased isotope uptake from rest to exercise and the blood pressure ratio was documented. Instead of ^{99m}Tc-sestamibi SPECT, ^{201}Tl perfusion scintigraphy was used in another report by Hamanaka et al., which also allowed for quantitative evaluation of intermittent claudication in patients [58].

^{99m}Tc-sestamibi was also used for evaluation of regional blood supply of thigh and calf muscles in early stages of atherosclerosis [59, 60]. A reduced stress and rest perfusion of lower limb muscles could be documented in clinically asymptomatic patients with atherosclerotic changes of lower limb vessels. Therefore, this technique could help early detection of the ischemic changes in asymptomatic patients, thereby enabling early intervention and prevention of disease progression.

^{99m}Tc-pyrophosphate has been used to estimate the ischemic skeletal muscle mass in ischemia-reperfusion injury [61]. In another report, ^{99m}Tc-pyrophosphate SPECT was employed to measure the amount of regional skeletal muscle necrosis in patients [62]. It was speculated that the volume of necrosis determined by this method could predict the clinical outcome. However, in a study by Bajnok et al., ^{99m}Tc-sestamibi was paradoxically taken up at a higher level in muscles supplied by significantly stenosed vessels [63]. In this study, muscle perfusion of lower extremities in 35 patients with peripheral vascular disease was functionally investigated, and the results of ^{99m}Tc-sestamibi scintigraphy were compared with those of angiography to estimate the diagnostic accuracy. The sensitivity and specificity of ^{99m}Tc-sestamibi scintigraphy were found to be 55% and 25%, respectively, with an overall accuracy of 50%. It was concluded that ^{99m}Tc-sestamibi scintigraphy was

not sufficiently reliable to improve the management of patients with peripheral vascular disease [63].

Conclusion and Future Perspectives

PET and SPECT are highly suitable for molecular imaging of angiogenesis since they are both tomographic and very sensitive. In addition, PET is also highly quantitative. Small animal PET/SPECT imaging has been widely used over the last decade in preclinical research [19]. PET is superior to SPECT in terms of higher sensitivity and more established attenuation correction algorithms, while SPECT can provide better spatial resolution than PET (applicable to dedicated small animal scanners but not clinical scanners) and allow for the use of multiple isotopes simultaneously [64]. Dual tracer imaging with SPECT can enable the investigation of different physiological and molecular functions (e.g., blood flow and angiogenesis) under the same physiological conditions, which is critical when the targets under investigation depend on each other hence requiring simultaneous assessment under identical conditions. A major limitation for PET/SPECT imaging of hindlimb ischemia with small molecule or peptide-based tracers is the intense accumulation of radioactivity in the bladder, which may hamper reliable analysis of the proximal hindlimb, located above the site of ligation of the femoral artery in the commonly used hindlimb ischemia model [49]. Further development and optimization of antibody and nanomaterial-based imaging agents may circumvent this problem because of the lack of renal clearance.

Antibody-based imaging has been a dynamic area of research over the last several decades [65, 66]. For example, an antibody which specifically binds to human and murine CD105 (i.e., TRC105, a human/murine chimeric IgG1 monoclonal antibody) has recently been investigated for molecular imaging of tumor angiogenesis, after it was labeled with various PET isotopes [67–70]. Similar as VEGFR and integrin $\alpha_v\beta_3$, CD105 also plays an important role in angiogenesis which is distinct from the VEGF/VEGFR pathway [71, 72]. Therefore, longitudinal imaging of CD105 expression in PAD models can give complementary information to the tracers discussed above. Recently, pilot studies in our laboratory have shown that ^{64}Cu-labeled TRC105 can be successfully used for noninvasive PET imaging of angiogenesis in the mouse hindlimb ischemia model (our unpublished data, Fig. 4), which warrants detailed investigation in the future and potential clinical translation.

Although the hindlimb ischemia model is well-established and commonly used for investigation of PAD, the expression of angiogenesis-related molecular markers and collateral vessel creation is dependent on the mouse strain and may vary in older, atherosclerotic, and hypercholesterolemic mice [73, 74]. Therefore, future studies are needed in animal models that better reflect the clinical situation and vascular status of PAD patients. Rapid translation of the promising PET/SPECT agents, not only some of those discussed above but also certain others under development, for clinical imaging of PAD is critical to the maximum benefit of patients.

Development of PET/SPECT tracers with relatively long decay half-lives (e.g., 12 h to a few days) may be more suitable for future clinical investigation with relatively low cost. A longer half-life can allow the production and transport of radiotracers from a single center to many other laboratories/clinics, obviating the establishment of an on-site cyclotron facility in every imaging center. The beauty of molecular imaging is that it is molecular specific, instead of disease specific. Since the biological process underlying PAD is related to various other cardiovascular diseases such as myocardial infarction, stroke, atherosclerosis, among others, the same tracers can also play important roles in the biomedical research of these diseases.

Acknowledgments

The authors acknowledge financial support from the University of Wisconsin Carbone Cancer Center, the Department of Defense (W81XWH-11-1-0644), and the Elsa U. Pardee Foundation.

References

1. Sumner AD, Khalil YK, Reed JF 3rd. The relationship of peripheral arterial disease and metabolic syndrome prevalence in asymptomatic US adults 40 years and older: results from the National Health and Nutrition Examination Survey (1999–2004). J Clin Hypertens (Greenwich). 2012; 14:144–8. [PubMed: 22372773]
2. van Weel V, van Tongeren RB, van Hinsbergh VW, van Bockel JH, Quax PH. Vascular growth in ischemic limbs: a review of mechanisms and possible therapeutic stimulation. Ann Vasc Surg. 2008; 22:582–97. [PubMed: 18504100]
3. Clair D, Shah S, Weber J. Current state of diagnosis and management of critical limb ischemia. Curr Cardiol Rep. 2012; 14:160–70. [PubMed: 22311595]
4. Hinchliffe RJ, Andros G, Apelqvist J, Bakker K, Friederichs S, Lammer J, et al. A systematic review of the effectiveness of revascularization of the ulcerated foot in patients with diabetes and peripheral arterial disease. Diabetes Metab Res Rev. 2012; 28 (Suppl 1):179–217. [PubMed: 22271740]
5. Ouriel K. Peripheral arterial disease. Lancet. 2001; 358:1257–64. [PubMed: 11675083]
6. Andersen CA. Noninvasive assessment of lower extremity hemodynamics in individuals with diabetes mellitus. J Vasc Surg. 2010; 52:76S–80S. [PubMed: 20804937]
7. Mathieu D, Mani R. A review of the clinical significance of tissue hypoxia measurements in lower extremity wound management. Int J Low Extrem Wounds. 2007; 6:273–83. [PubMed: 18048873]
8. Tang GL, Chin J, Kibbe MR. Advances in diagnostic imaging for peripheral arterial disease. Expert Rev Cardiovasc Ther. 2010; 8:1447–55. [PubMed: 20936931]
9. Galbraith JE, Murphy ML, de Soyza N. Coronary angiogram interpretation. Interobserver variability. JAMA. 1978; 240:2053–6. [PubMed: 702698]
10. Leape LL, Park RE, Bashore TM, Harrison JK, Davidson CJ, Brook RH. Effect of variability in the interpretation of coronary angiograms on the appropriateness of use of coronary revascularization procedures. Am Heart J. 2000; 139:106–13. [PubMed: 10618570]
11. Cavalcanti Filho JL, de Souza Leao Lima R, de Souza Machado Neto L, Kayat Bittencourt L, Domingues RC, da Fonseca LM. PET/CT and vascular disease: current concepts. Eur J Radiol. 2011; 80:60–7. [PubMed: 21371842]
12. Dobrucki LW, Sinusas AJ. Imaging angiogenesis. Curr Opin Biotechnol. 2007; 18:90–6. [PubMed: 17240135]
13. Suh JW, Scheinost D, Dione DP, Dobrucki LW, Sinusas AJ, Papademetris X. A non–rigid registration method for serial lower extremity hybrid SPECT/CT imaging. Med Image Anal. 2011; 15:96–111. [PubMed: 20869902]
14. Cai W, Chen X. Multimodality imaging of vascular endothelial growth factor and vascular endothelial growth factor receptor expression. Front Biosci. 2007; 12:4267–79. [PubMed: 17485373]
15. Cai W, Chen X. Multimodality molecular imaging of tumor angiogenesis. J Nucl Med. 2008; 49 (Suppl 2):113S–28S. [PubMed: 18523069]
16. Waters RE, Terjung RL, Peters KG, Annex BH. Preclinical models of human peripheral arterial occlusive disease: implications for investigation of therapeutic agents. J Appl Physiol. 2004; 97:773–80. [PubMed: 15107408]
17. Couffinhal T, Silver M, Zheng LP, Kearney M, Witzenbichler B, Isner JM. Mouse model of angiogenesis. Am J Pathol. 1998; 152:1667–79. [PubMed: 9626071]
18. Niiyama H, Huang NF, Rollins MD, Cooke JP. Murine model of hindlimb ischemia. J Vis Exp. 2009
19. James ML, Gambhir SS. A molecular imaging primer: modalities, imaging agents, and applications. Physiol Rev. 2012; 92:897–965. [PubMed: 22535898]

20. Ubbink DT, Tulevski, den Hartog D, Koelemay MJ, Legemate DA, Jacobs MJ. The value of non-invasive techniques for the assessment of critical limb ischaemia. Eur J Vasc Endovasc Surg. 1997; 13:296–300. [PubMed: 9129603]
21. Alauddin MM. Positron emission tomography (PET) imaging with ^{18}F-based radiotracers. Am J Nucl Med Mol Imaging. 2012; 2:55–76. [PubMed: 23133802]
22. Vach W, Høilund-Carlsen PF, Fischer BM, Gerke O, Weber W. How to study optimal timing of PET/CT for monitoring of cancer treatment. Am J Nucl Med Mol Imaging. 2011; 1:54–62. [PubMed: 23133795]
23. Zeman MN, Scott PJH. Current imaging strategies in rheumatoid arthritis. Am J Nucl Med Mol Imaging. 2012; 2:174–220. [PubMed: 23133812]
24. Bhargava P, He G, Samarghandi A, Delpassand ES. Pictorial review of SPECT/CT imaging applications in clinical nuclear medicine. Am J Nucl Med Mol Imaging. 2012; 2:221–31. [PubMed: 23133813]
25. Ogasawara Y, Ogasawara K, Suzuki T, Yamashita T, Kuroda H, Chida K, et al. Preoperative ^{123}I-iomazenil SPECT imaging predicts cerebral hyperperfusion following endarterectomy for unilateral cervical internal carotid artery stenosis. Am J Nucl Med Mol Imaging. 2012; 2:77–87. [PubMed: 23133803]
26. Stacy MR, Maxfield MW, Sinusas AJ. Targeted molecular imaging of angiogenesis in PET and SPECT: a review. Yale J Biol Med. 2012; 85:75–86. [PubMed: 22461745]
27. Gambhir SS, Czernin J, Schwimmer J, Silverman DH, Coleman RE, Phelps ME. A tabulated summary of the FDG PET literature. J Nucl Med. 2001; 42:1S–93S. [PubMed: 11483694]
28. Aparici CM, Carlson D, Nguyen N, Hawkins RA, Seo Y. Combined SPECT and Multidetector CT for Prostate Cancer Evaluations. Am J Nucl Med Mol Imaging. 2012; 2:48–54. [PubMed: 22267999]
29. Eary JF, Hawkins DS, Rodler ET, Conrad EUI. ^{18}F-FDG PET in sarcoma treatment response imaging. Am J Nucl Med Mol Imaging. 2011; 1:47–53. [PubMed: 23133794]
30. Gambhir SS. Molecular imaging of cancer with positron emission tomography. Nat Rev Cancer. 2002; 2:683–93. [PubMed: 12209157]
31. Grassi I, Nanni C, Allegri V, Morigi JJ, Montini GC, Castellucci P, et al. The clinical use of PET with ^{11}C-acetate. Am J Nucl Med Mol Imaging. 2012; 2:33–47. [PubMed: 23133801]
32. Zhao R, Wang J, Deng J, Yang W, Wang J. Efficacy of ^{99m}Tc-EDDA/HYNIC-TOC SPECT/CT scintigraphy in Graves' ophthalmopathy. Am J Nucl Med Mol Imaging. 2012; 2:242–7. [PubMed: 23133815]
33. Cai W, Rao J, Gambhir SS, Chen X. How molecular imaging is speeding up anti-angiogenic drug development. Mol Cancer Ther. 2006; 5:2624–33. [PubMed: 17121909]
34. Hao G, Hajibeigi A, De León-Rodríguez LM, Öz OK, Sun X. Peptoid-based PET imaging of vascular endothelial growth factor receptor (VEGFR) expression. Am J Nucl Med Mol Imaging. 2011; 1:65–75. [PubMed: 23133797]
35. Wang RE, Niu Y, Wu H, Amin MN, Cai J. Development of NGR peptide-based agents for tumor imaging. Am J Nucl Med Mol Imaging. 2011; 1:36–46. [PubMed: 23133793]
36. Zhang Y, Hong H, Engle JW, Yang Y, Barnhart TE, Cai W. Positron emission tomography and near-infrared fluorescence imaging of vascular endothelial growth factor with dual-labeled bevacizumab. Am J Nucl Med Mol Imaging. 2012; 2:1–13. [PubMed: 22229128]
37. Ferrara N. Vascular endothelial growth factor: basic science and clinical progress. Endocr Rev. 2004; 25:581–611. [PubMed: 15294883]
38. Ferrara N. VEGF and the quest for tumour angiogenesis factors. Nat Rev Cancer. 2002; 2:795–803. [PubMed: 12360282]
39. Cai W, Niu G, Chen X. Imaging of integrins as biomarkers for tumor angiogenesis. Curr Pharm Des. 2008; 14:2943–73. [PubMed: 18991712]
40. Almutairi A, Rossin R, Shokeen M, Hagooly A, Ananth A, Capoccia B, et al. Biodegradable dendritic positron-emitting nanoprobes for the noninvasive imaging of angiogenesis. Proc Natl Acad Sci USA. 2009; 106:685–90. [PubMed: 19129498]
41. Jeong JM, Hong MK, Chang YS, Lee YS, Kim YJ, Cheon GJ, et al. Preparation of a promising angiogenesis PET imaging agent: ^{68}Ga-labeled c(RGDyK)-isothiocyanatobenzyl-1,4,7-

triazacyclononane-1,4,7-triacetic acid and feasibility studies in mice. J Nucl Med. 2008; 49:830–6. [PubMed: 18413379]

42. Potter LR, Hunter T. Guanylyl cyclase-linked natriuretic peptide receptors: structure and regulation. J Biol Chem. 2001; 276:6057–60. [PubMed: 11152699]
43. van den Akker F. Structural insights into the ligand binding domains of membrane bound guanylyl cyclases and natriuretic peptide receptors. J Mol Biol. 2001; 311:923–37. [PubMed: 11556325]
44. Liu Y, Pressly ED, Abendschein DR, Hawker CJ, Woodard GE, Woodard PK, et al. Targeting angiogenesis using a C-type atrial natriuretic factor-conjugated nanoprobe and PET. J Nucl Med. 2011; 52:1956–63. [PubMed: 22049461]
45. Cai W, Hong H. Peptoid and positron emission tomography: an appealing combination. Am J Nucl Med Mol Imaging. 2011; 1:76–9. [PubMed: 22022661]
46. Willmann JK, Chen K, Wang H, Paulmurugan R, Rollins M, Cai W, et al. Monitoring of the biological response to murine hindlimb ischemia with ^{64}Cu-labeled vascular endothelial growth factor-121 positron emission tomography. Circulation. 2008; 117:915–22. [PubMed: 18250264]
47. Penuelas I, Aranguren XL, Abizanda G, Marti-Climent JM, Uriz M, Ecay M, et al. ^{13}N-ammonia PET as a measurement of hindlimb perfusion in a mouse model of peripheral artery occlusive disease. J Nucl Med. 2007; 48:1216–23. [PubMed: 17574988]
48. Hua J, Dobrucki LW, Sadeghi MM, Zhang J, Bourke BN, Cavaliere P, et al. Noninvasive imaging of angiogenesis with a ^{99m}Tc-labeled peptide targeted at alphavbeta3 integrin after murine hindlimb ischemia. Circulation. 2005; 111:3255–60. [PubMed: 15956134]
49. Dobrucki LW, Dione DP, Kalinowski L, Dione D, Mendizabal M, Yu J, et al. Serial noninvasive targeted imaging of peripheral angiogenesis: validation and application of a semiautomated quantitative approach. J Nucl Med. 2009; 50:1356–63. [PubMed: 19617325]
50. Depairon M, De Landsheere C, Merlo P, Del Fiore G, Quaglia L, Peters JM, et al. Effect of exercise on the leg distribution of $C^{15}O_2$ and $^{15}O_2$ in normals and in patients with peripheral ischemia: a study using positron tomography. Int Angiol. 1988; 7:254–7. [PubMed: 3264317]
51. Depairon M, Depresseux JC, De Landsheere C, Merlo P, Del Fiore G, Quaglia L, et al. Regional blood flow and oxygen consumption in the leg muscles of normal subjects and in those with arterial insufficiency. Study of the distribution of $C^{15}O_2$ and of $^{15}O_2$ using positron emission tomography. J Mal Vasc. 1988; 13:107–15. [PubMed: 3260934]
52. Keenan GF, Ashcroft GP, Roditi GH, Hutchison JD, Evans NT, Mikecz P, et al. Measurement of lower limb blood flow in patients with neurogenic claudication using positron emission tomography. Spine (Phila Pa 1976). 1995; 20:408–11. [PubMed: 7747223]
53. Scremin OU, Figoni SF, Norman K, Scremin AM, Kunkel CF, Opava-Rutter D, et al. Preamputation evaluation of lower-limb skeletal muscle perfusion with $H_2{}^{15}O$ positron emission tomography. Am J Phys Med Rehabil. 2010; 89:473–86. [PubMed: 20357647]
54. Nawaz A, Saboury B, Basu S, Zhuang H, Moghadam-Kia S, Werner T, et al. Relation Between Popliteal-Tibial Artery Atherosclerosis and Global Glycolytic Metabolism in the Affected Diabetic Foot: A Pilot Study Using Quantitative FDG-PET. J Am Podiatr Med Assoc. 2012; 102:240–6. [PubMed: 22659767]
55. Nolting DD, Nickels ML, Guo N, Pham W. Molecular imaging probe development: a chemistry perspective. Am J Nucl Med Mol Imaging. 2012; 2:273–306. [PubMed: 22943038]
56. Beller GA, Sinusas AJ. Experimental studies of the physiologic properties of technetium-99m isonitriles. Am J Cardiol. 1990; 66:5E–8E.
57. Bostrom PA, Diemer H, Leide S, Lilja B, Bergqvist D. ^{99m}Tc-sestamibi uptake in the leg muscles and in the myocardium in patients with intermittent claudication. Angiology. 1993; 44:971–6. [PubMed: 8285375]
58. Hamanaka D, Odori T, Maeda H, Ishii Y, Hayakawa K, Torizuka K. A quantitative assessment of scintigraphy of the legs using ^{201}Tl. Eur J Nucl Med. 1984; 9:12–6. [PubMed: 6230235]
59. Kusmierek J, Dabrowski J, Bienkiewicz M, Szuminski R, Plachcinska A. Radionuclide assessment of lower limb perfusion using ^{99m}Tc-MIBI in early stages of atherosclerosis. Nucl Med Rev Cent East Eur. 2006; 9:18–23. [PubMed: 16791799]

60. Miles KA, Barber RW, Wraight EP, Cooper M, Appleton DS. Leg muscle scintigraphy with ^{99m}Tc-MIBI in the assessment of peripheral vascular (arterial) disease. Nucl Med Commun. 1992; 13:593–603. [PubMed: 1513521]
61. Forrest I, Hayes G, Smith A, Yip TC, Walker PM. Identification of clinically significant skeletal muscle necrosis by single photon emission computed tomography. Can J Surg. 1989; 32:109–12. [PubMed: 2537678]
62. Yip TC, Houle S, Tittley JG, Walker PM. Quantification of skeletal muscle necrosis in the lower extremities using ^{99m}Tc pyrophosphate with single photon emission computed tomography. Nucl Med Commun. 1992; 13:47–52. [PubMed: 1534397]
63. Bajnok L, Kozlovszky B, Varga J, Antalffy J, Olvaszto S, Fulop T Jr. Technetium-99m sestamibi scintigraphy for the assessment of lower extremity ischaemia in peripheral arterial disease. Eur J Nucl Med. 1994; 21:1326–32. [PubMed: 7875171]
64. Dobrucki LW, Sinusas AJ. PET and SPECT in cardiovascular molecular imaging. Nat Rev Cardiol. 2010; 7:38–47. [PubMed: 19935740]
65. Wu AM. Antibodies and antimatter: the resurgence of immuno-PET. J Nucl Med. 2009; 50:2–5. [PubMed: 19091888]
66. Wu AM, Senter PD. Arming antibodies: prospects and challenges for immunoconjugates. Nat Biotechnol. 2005; 23:1137–46. [PubMed: 16151407]
67. Zhang Y, Hong H, Engle JW, Yang Y, Theuer CP, Barnhart TE, et al. Positron emission tomography and optical imaging of tumor CD105 expression with a dual-labeled monoclonal antibody. Mol Pharm. 2012; 9:645–53. [PubMed: 22292418]
68. Hong H, Severin GW, Yang Y, Engle JW, Zhang Y, Barnhart TE, et al. Positron emission tomography imaging of CD105 expression with ^{89}Zr-Df-TRC105. Eur J Nucl Med Mol Imaging. 2012; 39:138–48. [PubMed: 21909753]
69. Zhang Y, Hong H, Engle JW, Bean J, Yang Y, Leigh BR, et al. Positron emission tomography imaging of CD105 expression with a ^{64}Cu-labeled monoclonal antibody: NOTA is superior to DOTA. PLoS One. 2011; 6:e28005. [PubMed: 22174762]
70. Engle JW, Hong H, Zhang Y, Valdovinos HF, Myklejord DV, Barnhart TE, et al. Positron emission tomography imaging of tumor angiogenesis with a ^{66}Ga-labeled monoclonal antibody. Mol Pharm. 2012; 9:1441–8. [PubMed: 22519890]
71. Dallas NA, Samuel S, Xia L, Fan F, Gray MJ, Lim SJ, et al. Endoglin (CD105): a marker of tumor vasculature and potential target for therapy. Clin Cancer Res. 2008; 14:1931–7. [PubMed: 18381930]
72. Zhang Y, Yang Y, Hong H, Cai W. Multimodality molecular imaging of CD105 (Endoglin) expression. Int J Clin Exp Med. 2011; 4:32–42. [PubMed: 21394284]
73. Helisch A, Wagner S, Khan N, Drinane M, Wolfram S, Heil M, et al. Impact of mouse strain differences in innate hindlimb collateral vasculature. Arterioscler Thromb Vasc Biol. 2006; 26:520–6. [PubMed: 16397137]
74. Tirziu D, Moodie KL, Zhuang ZW, Singer K, Helisch A, Dunn JF, et al. Delayed arteriogenesis in hypercholesterolemic mice. Circulation. 2005; 112:2501–9. [PubMed: 16230502]
75. Saucy F, Dischl B, Delachaux A, Feihl F, Liaudet L, Waeber B, et al. Foot skin blood flow following infrainguinal revascularization for critical lower limb ischemia. Eur J Vasc Endovasc Surg. 2006; 31:401–6. [PubMed: 16359880]
76. Murohara T, Asahara T, Silver M, Bauters C, Masuda H, Kalka C, et al. Nitric oxide synthase modulates angiogenesis in response to tissue ischemia. J Clin Invest. 1998; 101:2567–78. [PubMed: 9616228]

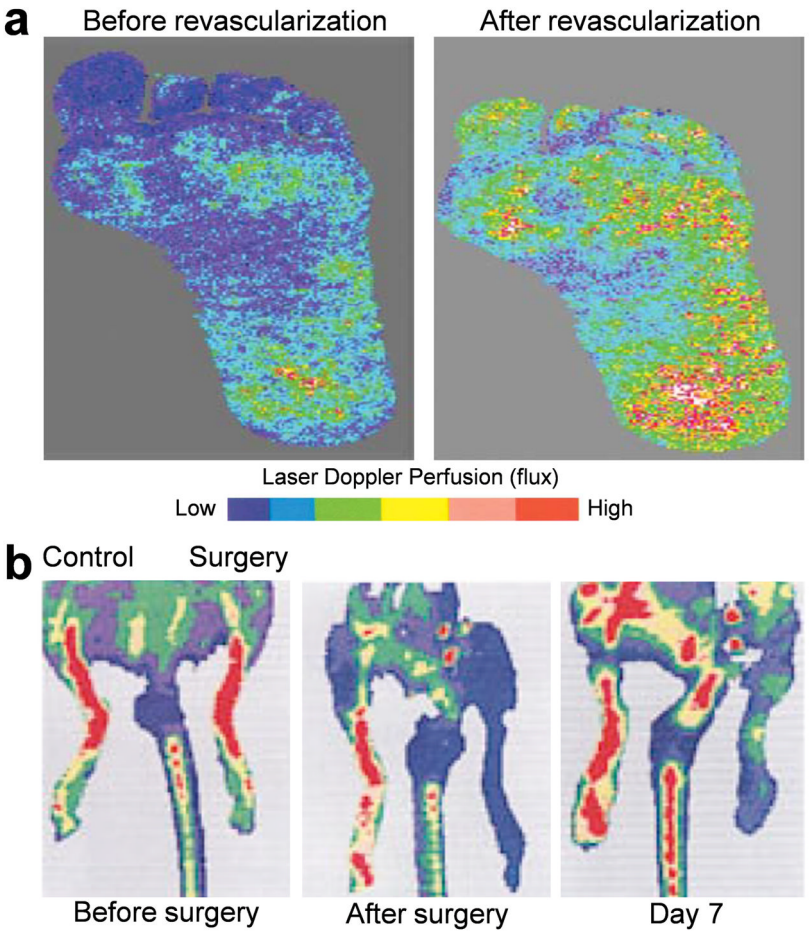

Fig. 1.

a Laser Doppler imaging of the ischemic foot of a patient with diabetes before and after infrainguinal revascularization. The areas with improved perfusion are shown in red and the areas with poor perfusion are shown in blue. **b** Serial laser Doppler imaging of ischemic hindlimb of a C57 mouse. Decreased perfusion soon after the surgery (dark blue) was observed in the ischemic limb, whereas high perfusion pattern (red to orange) was detected in the control hindlimb. The recovery of perfusion was clearly detectable on day 7. Adapted from [75, 76].

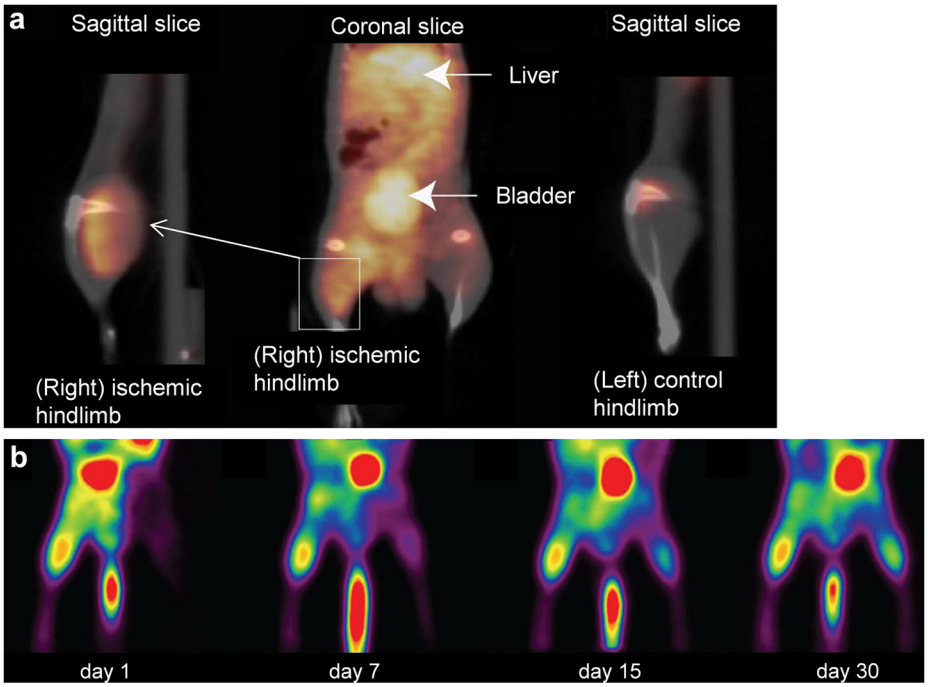

Fig. 2.

a Noninvasive PET/CT images of angiogenesis in a murine hindlimb ischemia model. An integrin $\alpha_v\beta_3$-targeted dendritic nanoprobe had significantly higher uptake in the ischemic hindlimb than the control hindlimb. **b** Serial ^{13}N-ammonia PET images of spontaneous perfusion recovery in a murine hindlimb ischemia model, at different time points after surgery. Adapted from [40, 47].

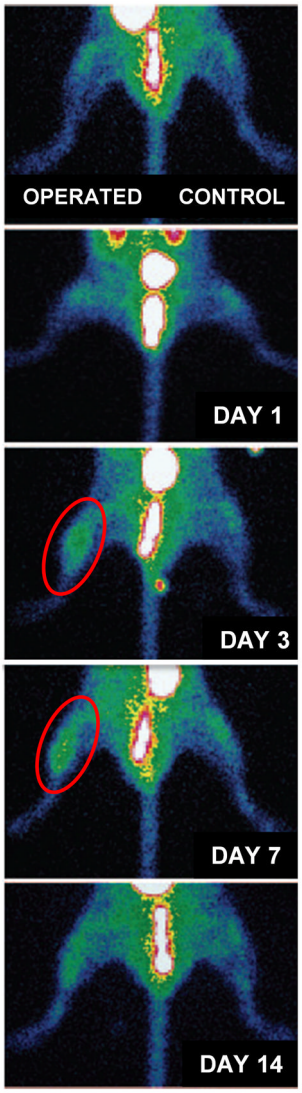

Fig. 3.

In vivo planar pinhole images of ischemic hindlimb of a mouse at various time points after surgery, after intravenous injection of ^{99m}Tc-NC100692. A significant increase in tracer uptake in the ischemic hindlimb was observed on days 3 and 7 after surgery (red circle). Adapted from [48].

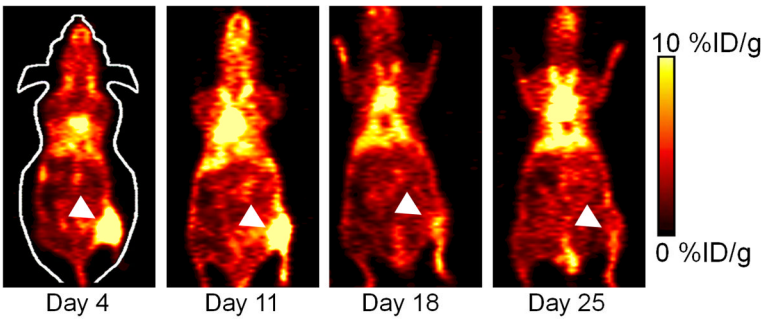

Fig. 4.

Serial PET imaging of CD105 expression in a murine hindlimb ischemia model at different days after surgery, acquired at 48 h post-injection of ^{64}Cu-NOTA-TRC105. The white arrowheads indicate increased uptake in the ischemic hindlimb, which returned to background level on day 25.

Table 1

A tabulated summary of PET/SPECT imaging of hindlimb/extremity ischemia.

	PET	SPECT
Angiogenesis targeted	^{76}Br-nanoprobe [40]	^{99m}Tc-NC100692 [48, 49]
	^{68}Ga-NOTA-RGD [41]	
	^{64}Cu-DOTA-CANF-comb [44]	
	^{64}Cu-DOTA-VEGF$_{121}$ [46]	
	^{64}Cu-NOTA-TRC105	
Blood flow	^{13}N-ammonia [47]	^{99m}Tc-sestamibi [57, 59, 60, 63]
	C^{15}O$_2$ and ^{15}O$_2$ [50, 51]	^{99m}Tc-pyrophosphate [61, 62]
	H$_2$^{15}O [52, 53]	^{201}Tl [58]
	^{18}F-FDG [54]	